Macromolecules
ARTICLE

Macromolecules **2009**, *42*, 8385–8391 **8385**
DOI: 10.1021/ma901399v

Transition Behavior of Weakly Interacting PS-*b*-PMMA Films on Preferential Surfaces: A Direct Observation by GISAXS

Eunhye Kim,[†] Hyungju Ahn,[†] Du Yeol Ryu,*[,†] Jehan Kim,[‡] and Junhan Cho*[,§]

[†]*Department of Chemical and Biomolecular Engineering, Yonsei University, Seoul 120-749, Korea,* [‡]*Beamline Department, Pohang Accelerator Laboratory, Pohang 790-784, Korea, and* [§]*Department of Polymer Science & Engineering and Center for Photofunctional Energy Materials, Dankook University, Yongin, Gyeonggi-do 448-701, Korea*

Received June 30, 2009; Revised Manuscript Received September 30, 2009

ABSTRACT: The phase transitions for the films of a symmetric polystyrene-*b*-poly(methyl methacryltate) (PS-*b*-PMMA) on a modified surface, like the order-to-disorder transition (ODT) in the weak segregation regime, was investigated by *in situ* grazing incidence small-angle X-ray scattering (GISAXS). The selective interactions at the surface by PS-brush substrate that favors the preferential interactions with the PS component of the block copolymer enhance the parallel orientation of the lamellar microdomains to the film surface. This effect for weakly interacting PS-*b*-PMMA films leads to a gentle decrease of the transition temperature with increasing film thickness up to $50L_0$ (lamellar period). We discuss this thickness dependence of transition temperatures for PS-*b*-PMMA films on preferential surfaces in terms of the temperature dependence of χ between two block components.

Introduction

The thin films of block copolymer (BCP), consisting of chemically different polymers covalently linked together, have received attention as promising templates and scaffolds in tens of nanometers, since BCP can self-assemble into the ordered nanostructures such as lamellar, cylindrical, gyroid, and spherical arrays on the substrates.[1,2] Some research efforts for various applications of BCP films have stimulated the studies on the controlled interfacial interactions and the confinement at the interfaces to facilitate the microdomain orientation for the desired practical uses.[3−16] The preferential interaction of one block component with substrate and/or the difference of surface tension between two block components can lead to the parallel orientation of lamellar microdomains in the vicinity of two interfaces at the substrate/polymer and polymer/air.[3−6] In contrast, the balanced interfacial interactions (on the neutral substrate) enable BCP microdomains to orient normal to the film surface.[7−12] It is, therefore, of great importance to understand the phase behavior in film geometry that confines polymer chains to the interfaces, which would be expected to differ appreciably from that in the bulk state.[17,18]

A classic order−disorder transition (ODT) behavior of BCP can be determined at a temperature of T_{ODT} from the ordered to the disordered (or physically phase-mixed) state when the enthalpic term of free energy of mixing is equal to the entropic term. As for a symmetric BCP of $\chi N > 10.495$, the microphase separation occurs, where χ is the segmental interaction parameter as a function of temperature (T) and N is the overall number of segments in the BCP.[19,20] Hence, an ODT-type BCP where χ is proportional to $1/T$ shows the microphase separation upon cooling and the phase mixing at elevated temperature.

It has been reported that the transition in BCP films, unlike that in the bulk state, can be influenced by the interfacial interactions.[21−24] The transition behavior for the films of symmetric polystyrene-*b*-deuterated poly(methyl methacryltate) (PS-*b*-dPMMA) on Si substrates was first studied by *ex situ* neutron reflectivity (NR) as a function of temperature and film thickness, leading to the thickness dependence on T_∞, where T_∞ is a temperature when the decay length (ξ) reduces discontinuously with increasing temperature and approaches to infinity.[21] This transition temperature was defined as the order-to-a partial disorder transition rather than ODT, since the scattering length density above T_{ODT} of the bulk state never achieved a constant value equal to the average value of two components. It indicates that the periodic ordered layers remains at the interfaces of the substrate and the top, while the middle of the film still is disordered.[22]

A field-theoretic simulation study of BCP confined between two neutral walls showed that the ODT by taking the fluctuation effect into account is strongly suppressed for L_0 (lamellar period) < 1 but consistently shifted up to 10% with respect to the mean-field value of $\chi N = 10.495$, which is in agreement with the analytical study on the confinement effect of ODT in the BCP melts.[25,26] This result also represents that the phase transition of BCP in film geometry can be significantly influenced by the interfacial interactions.

Recently, the phase transitions for the films of a lamella-forming polystyrene-*b*-polyisoprene (PS-*b*-PI) on preferential surfaces was investigated by *in situ* grazing incidence small-angle X-ray scattering (GISAXS) in comparison to that for the bulk state.[23] The thickness dependence of transition temperatures, as a consequence of the suppression of the compositional fluctuations, leads to a characteristic thickness of $\sim 12L_0$ where the transition temperature begins to significantly increase with decreasing film thickness. Hence, for the film less than $12L_0$, the T_{ODT} increases drastically with decreasing film thickness because the strength of interfacial interactions is inversely proportional to the film thickness. It should be pointed out that PS-*b*-PI possesses a strong temperature dependence on χ, indicating a drastic change with thermal energy.

To elucidate the effect of temperature dependence on χ for the transition behavior of BCP films in the weak segregation regime,

*To whom correspondence should be addressed. E-mail: dyryu@yonsei.ac.kr (D.Y.R), jhcho@dku.edu (J.C).

Published on Web 10/15/2009

in this study, we focused on the phase transitions for the films of lamella-forming polystyrene-*b*-poly(methyl methacryltate) (PS-*b*-PMMA) on preferential surfaces as a weakly interacting BCP with a weak temperature dependence of χ. The thickness dependence of transition temperatures for PS-*b*-PMMA films leads experimentally to a gentle decrease of the transition temperature with increasing film thickness up to $50L_0$ (lamellar period), which is still above the order-to-disorder transition temperature (T_{ODT}) for the bulk PS-*b*-PMMA. This result is systematically compared to the transition behaviors calculated by the mean-field theory depending on the relative magnitude of enthalpic contribution (temperature-dependent part) to χ.

Experimental Section

A nearly symmetric PS-*b*-PMMA used in this study was purchased from Polymer Source, which was synthesized by the sequential anionic polymerization of styrene and methyl methacrylate in tetrahydrofuran (THF) at −78 °C in the presence of LiCl using *sec*-butyllithium as an initiator. The number-average molecular weight (M_n) and polydispersity index (PDI), characterized by size-exclusion chromatography (SEC), were measured to be 29 000 g/mol and 1.08, respectively. PS volume fraction (Φ_{PS}) of BCP was determined to be 0.553 by ^{1}H nuclear magnetic resonance (^{1}H NMR) based on the mass densities of two components (1.05 and 1.184 g/cm^3 for PS and PMMA). A hydroxyl-terminated polystyrene (PS-OH) was synthesized via anionic polymerization (Polymer Source), having M_n = 10 000 and PDI = 1.07.

To prepare a selectively preferential PS-brush surface, a thin film of PS-OH by spin-coating on the standard Si substrate from the solution in toluene was annealed at 170 °C under vacuum for 3 days. During annealing well above the glass transition temperatures (T_g) of PS (< 100 °C), end-functional hydroxyl groups of PS-OH diffuse to and react with the native oxide layer. After rinsing with toluene to remove the nonanchored chains, the thickness of PS-brush was measured to be 5.0 ± 0.3 nm by ellipsometry (SE MG-1000, Nanoview Co.).

A given amount of PS-*b*-PMMA was dissolved in toluene and spin-coated onto the PS-brush substrate that was cleaned with toluene and dried with a stream of nitrogen before use. Subsequently, the BCP films were annealed at 170 °C under vacuum for 3 days to allow the thermal equilibrium above T_g's for PS and PMMA (100 and 115 °C, respectively). The thicknesses of BCP films were controlled by spin-coating at high speed (4000 rpm) from 196 nm ($10L_0$) to 980 nm ($50L_0$), where L_0 (= 19.6 nm) is consistent with *d*-spacing at 170 °C in the bulk state, determined by $d = 2\pi/q^*$.

Synchrotron scattering experiments were conducted to probe the transition temperatures at 4C1 for small-angle X-ray scattering (SAXS) and 4C2 (GISAXS) beamlines of the Pohang Accelerator Laboratory (PAL), Korea.[27] The operating conditions for GISAXS were set to a wavelength of 1.38 Å and the sample-to-detector distance of 2.2 m. The film samples were mounted on a heating cell under vacuum, and the incident angle was set at 0.16°−0.18°, which is above the critical angle (0.156°) of PS-*b*-PMMA films.[28] For BCP films, this technique has recently provided the detailed analysis with the characteristic patterns of nanostructures by virtue of the large scattering volume,[28−32] whereas X-ray reflectivity allows a mean value of electron densities for two components due to the lack of the contrast between two components.[33] 2D GISAXS patterns were recorded using a CCD detector (Princeton Instruments) positioned at the end of a vacuum guide tube when the X-ray beam pass through the BCP films under vacuum. The least exposure time and frequency were used so as to avoid the sample degradation by X-rays. SAXS was measured to determine the bulk behavior of the BCP. All the heating experiments were automatically controlled with a PID temperature controller from 150 to 245 °C at a constant heating rate of 0.9 °C/min and with the exposure time of 10−60 s.

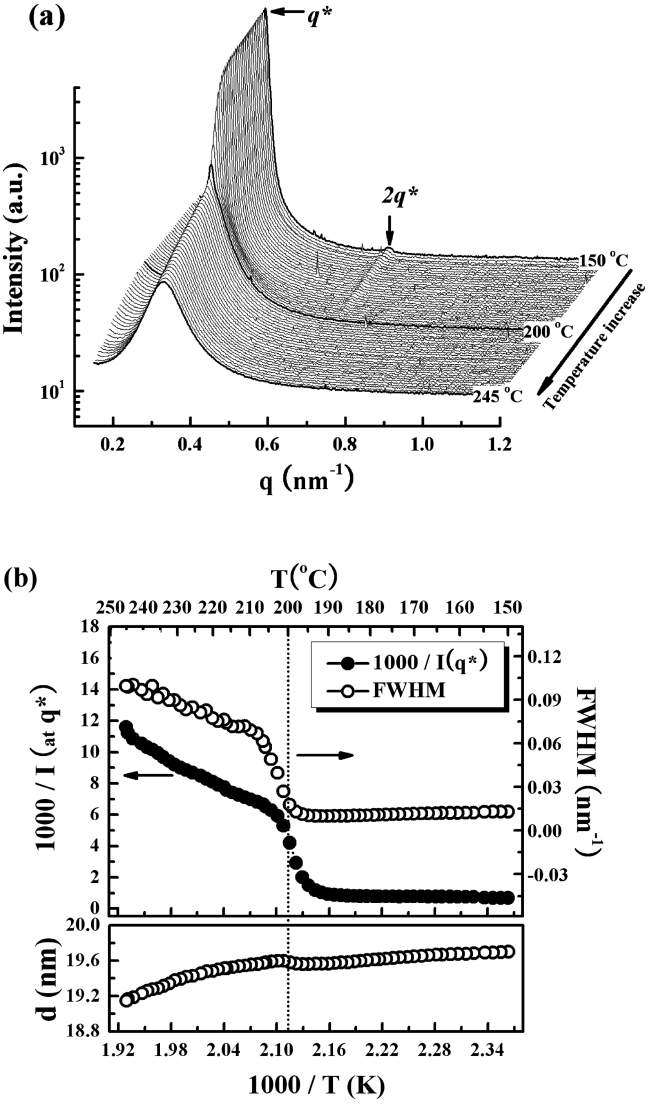

Figure 1. (a) SAXS intensity profiles for the bulk PS-*b*-PMMA as a function of scattering vector (q) at various temperatures during heating at a rate of 0.9 °C/min from 150 to 245 °C and (b) the scattering parameters derived from SAXS profiles. The inverse of the maximum intensity ($1/I(q_{max})$), full width at half-maximum (fwhm), and *d*-spacing by $d = 2\pi/q^*$ are plotted as a function of inverse temperature (1/K). Arrows indicate the first-order peak at $q^* = 0.319$ nm^{-1} and the second-order peak at $2q^*$.

Results and Discussion

SAXS intensity profiles for PS-*b*-PMMA reflecting the phase structures in the bulk state, measured at various temperatures during heating at a rate of 0.9 °C /min from 150 to 245 °C, are shown in Figure 1a as a function of the scattering vector (q), where $q = (4\pi/\lambda) \sin\theta$; 2θ and λ are the scattering angle and wavelength, respectively. At low temperatures (T < 200 °C), a sharp scattering peak located at $q^* = 0.319$ nm^{-1} and the second-order peak at $2q^*$ relative to the first-order reflection (indicated by arrows), the characteristic of the lamellar microdomain morphology, are observed due to the microphase separation by the unfavorable segmental interactions between two block components. Here, only discernible higher order peak to $2q^*$ is caused by the low contrast in electron densities between two components of PS-*b*-PMMA. With increasing temperature (T > 200 °C), the primary peak significantly weakens and broadens and then maintains a diffuse maximum with no second-order peak. The diffuse scattering at higher temperature corresponds to the

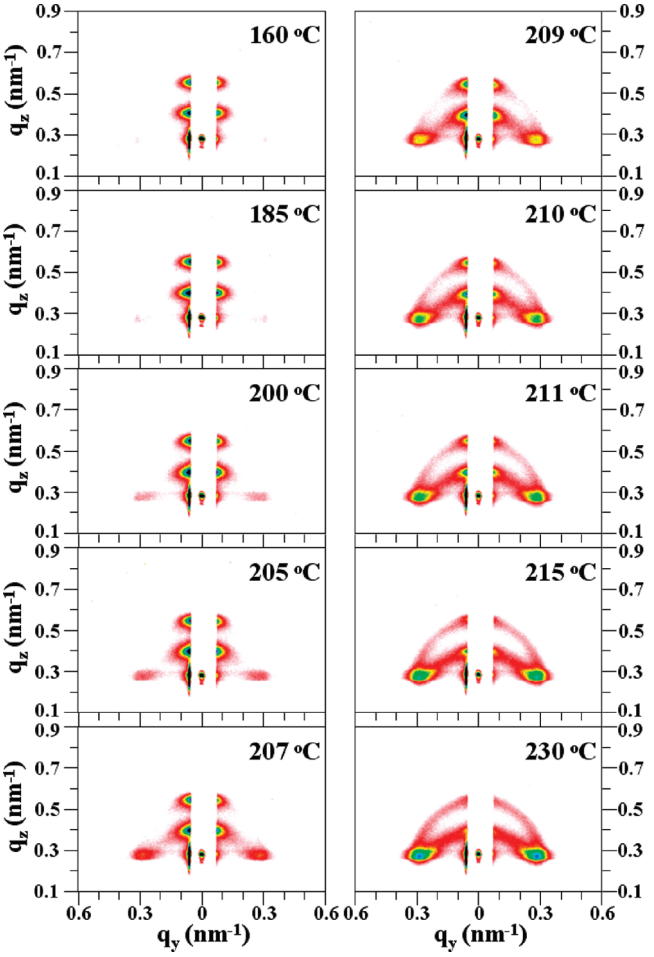

Figure 2. 2D GISAXS patterns for PS-*b*-PMMA film of $40L_0$ (785 nm) on PS-brush substrate at incident angle of 0.17°, which is above the critical angle (0.156°) of PS-*b*-PMMA films. All patterns were taken at each temperature during heating from 160 to 230 °C at a rate of 0.9 °C/min after thermally annealing the film at 170 °C for 3 days under vacuum.

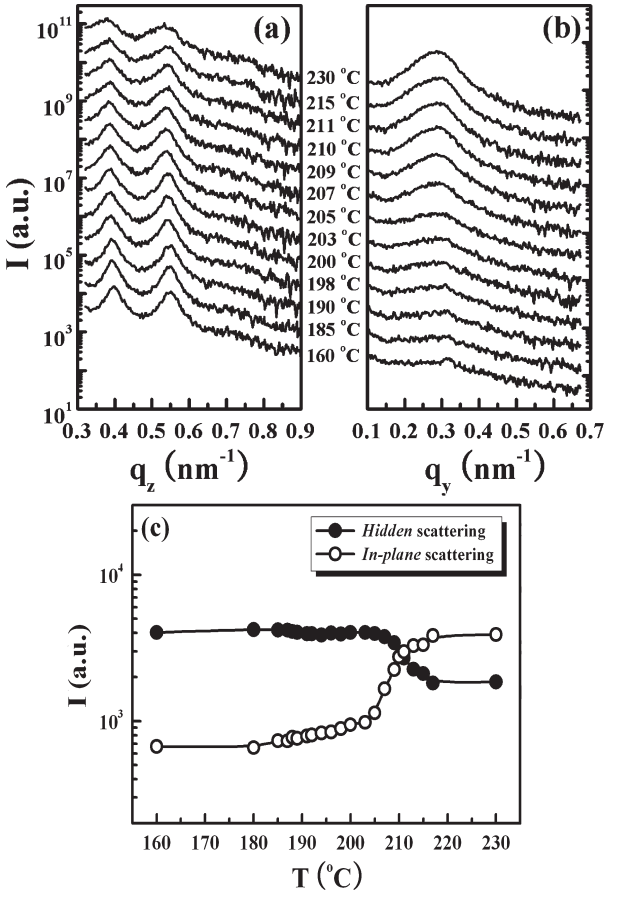

Figure 3. Intensity profiles from the GISAXS patterns in Figure 2 for PS-*b*-PMMA film of $40L_0$ at both (a) the *hidden* scattering scanned along the q_z direction near $q_y = 0$ (the vertical beamstop) during heating and (b) the *in-plane* scattering scanned along the q_y direction at constant $q_z = 0.269$ nm^{-1} (corresponding to q_z of the reflected beam), respectively. Intensities were rescaled with the shift factor of 3−4. (c) Maximum intensities of both peaks as a function of temperature. By the discontinuity in intensities, the parallel orientation of the lamellar microdomains on PS-brush substrate disappears into the disordered state in film at greater than 209 °C.

characteristic correlation hole scattering of the disordered (or phase-mixed) BCP, which arises from the compositional fluctuations of two connecting components in the R_g (radius of gyration) length scale.[19] This behavior is typical for ODT-type BCPs undergoing a transition from the ordered to disordered state with temperature. Accordingly, one can readily determine an order-to-disorder transition (T_{ODT}) at 200±5 °C for PS-*b*-PMMA by the discontinuous changes of the scattering parameters derived from the SAXS profiles, such as the inverse of the maximum intensity ($1/I(q^*)$), full width at half-maximum (fwhm), and *d*-spacing (*d*) by $d = 2\pi/q^*$ as a function of inverse temperature (1/K), as plotted in Figure 1b. As temperature increases over T_{ODT}, $1/I(q^*)$ and fwhm increase and *d*-spacing gradually decreases, where the interaction parameter (χ) between two block components decreases proportionally to T and the thermal fluctuation increases. It should be mentioned that a broader transition range (195−205 °C) can be correlated to the weak temperature dependence (or small enthalpic contribution) on $\chi = 0.0282 + 4.46/T$ for PS-*b*-PMMA,[34] compared with the strong temperature dependence on $\chi = -0.0419 + 38.54/T$ for PS-*b*-PI.[35]

Figure 2 shows *in situ* 2D GISAXS patterns for PS-*b*-PMMA film with thickness of 785 nm on PS-brush substrate, at which the patterns were taken at each temperature during heating from 160 to 230 °C at a rate of 0.9 °C/min after thermally annealing the film at 170 °C for 3 days under vacuum. This thickness corresponds to $40L_0$, where L_0 is the interlamellar spacing or *d*-spacing ($d = 2\pi/q^*$) of 19.6 nm, taken at the ordered state of bulk PS-*b*-PMMA at 160 °C. The least exposure time at the selective temperatures was used in order to avoid X-ray beam damages that can influence the transition temperature. In the scattering geometry used, q_y is the scattering vector normal to the incident plane, which is related to *d*-spacing of the film by $d = 2\pi/q_y$, and q_z is the scattering vector normal to the sample surface, defined as $q_z = (4\pi/\lambda)\sin\theta$. In order to probe the morphology of the entire film, the incidence angle was set at 0.17° above the critical angle (0.156°) of PS-*b*-PMMA films.[28,29]

For the GISAXS pattern at $T = 160$ °C, two strong scattering peaks along q_z near $q_y = 0$ (or the vertical beamstop) are distinct, hereafter denoted as the *hidden* scattering, and little *in-plane* scattering peaks are perceptible along q_y at constant $q_z = 0.269$ nm^{-1} (corresponding to q_z of the reflected beam). This characteristic pattern corresponds to the interfaces for the multilayered lamellar microdomains aligned parallel to the film surface,[36,37] in good agreement with the recent report on the films of lamellar-forming PS-*b*-PI.[23] The parallel orientation of the lamellar microdomains can be attributed to the selective interactions on PS-brush substrate to the PS component of the BCP, causing near the substrate the high concentration of PS block chains that can lead to the compositional propagation into the film, evidenced by the

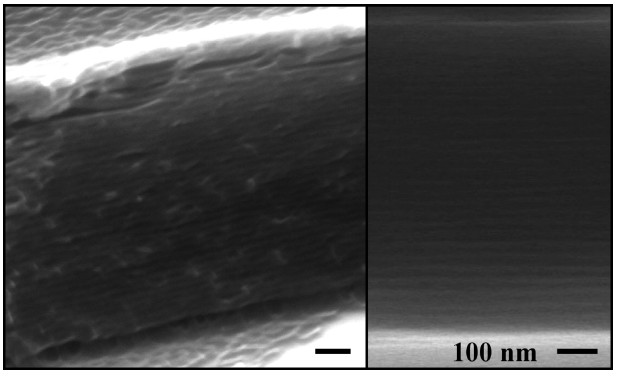

Figure 4. SEM images for PS-*b*-PMMA film of $40L_0$ on PS-brush substrate, which were taken by quenching after thermally annealing the film at 170 °C for 3 days under vacuum. The left and right images was taken at a tilt angle of 55° after etching PMMA component and cross-sectional view with no etching, respectively.

SEM images in Figure 4 (will be discussed later). The similar GISAXS patterns are shown in the film even up to 205 °C, which is higher than the T_{ODT} (200 °C) of the bulk PS-*b*-PMMA, although the *in-plane* scattering peaks weakly appear. With further increasing temperature (T > 209 °C), the *in-plane* scattering peaks intensify and reach a weak and broad maximum up to 230 °C at the expense of the *hidden* scattering peaks, indicating the disordering of BCP films at higher temperature. Two elliptical diffuse scattering patterns observed for T > 209 °C from the reflected and transmitted X-ray beams confirm a disordered BCP film, which arise from a superposition of the correlation hole scatterings by the compositional fluctuations in the films. Upon direct cooling to 160 °C, the *hidden* scattering peaks reappear, and the *in-plane* scattering peaks gradually weaken but still remain in 1 h due to insufficient annealing time for the thermal equilibrium (not shown here).

To determine the transition temperature in the BCP film quantitatively, the intensity profiles from the GISAXS patterns in Figure 2 are scanned along the q_z direction near the vertical beamstop (q_y = 0) and along the q_y direction at constant q_z = 0.269 nm^{-1}, as shown in parts a and b of Figure 3, respectively. Over the temperatures from 160 to 230 °C, the *hidden* scattering peaks at the ordered state (T < 209 °C) in Figure 3a are much sharper than the *in-plane* scattering peaks at the disordered state (T > 209 °C) in Figure 3b, reflecting the structural changes of the entire film during heating. Hence, these complementary temperature dependences of both peak intensities enable us to efficiently determine the transition temperature in the BCP film, as plotted in Figure 3c, which are reasonably consistent with the direct analysis of the GISAXS patterns. Two discontinuous changes by an increase of *in-plane* scattering and a decrease of *hidden* scattering are observed at 209 ± 4 °C as a T_{ODT} of PS-*b*-PMMA film of $40L_0$. The similar transition temperatures were measured for PS-*b*-PMMA films of $32L_0$ (628 nm) and $50L_0$ (980 nm) on the PS-brush substrate, which are still above the T_{ODT} (200 °C) of the bulk PS-*b*-PMMA. This behavior can be a consequence of the suppression of compositional fluctuations by the pinned high concentration of PS block chains near the PS-brush substrate, which would be evidenced by the compositional propagation into the film where the lamellar microdomains orient parallel to the film surface.[23]

Figure 4 depicts the SEM images for PS-*b*-PMMA film of $40L_0$ after thermally annealing the film at 170 °C for 3 days under vacuum. The left image was taken at a tilt angle of 55°, where the PMMA microdomains were removed by UV exposure and subsequent rinsing with acetic acid shortly to enhance the contrast, indicating the parallel orientation of the lamellar microdomains

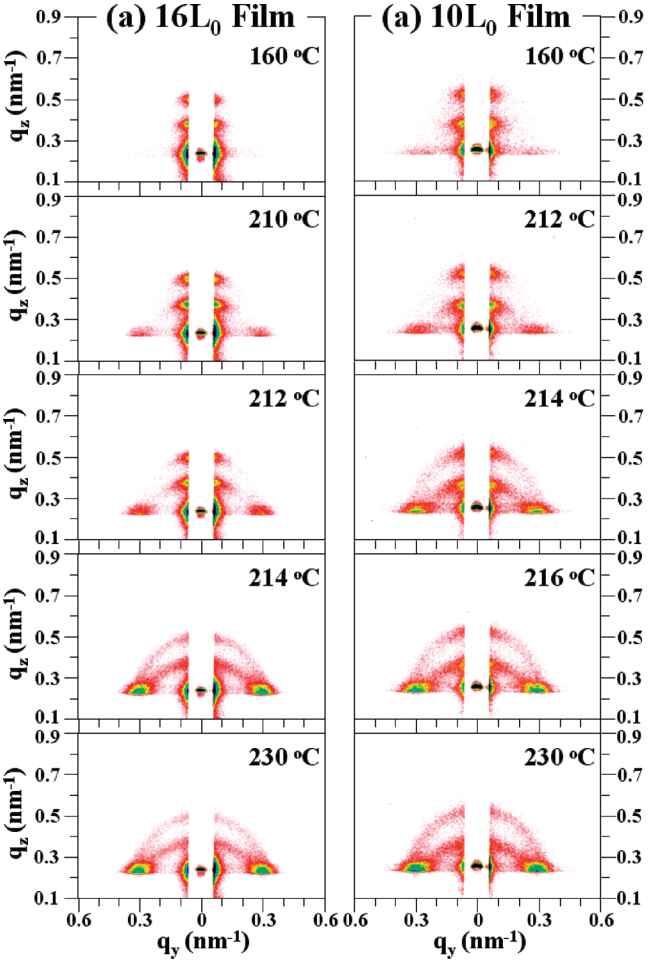

Figure 5. 2D GISAXS patterns for PS-*b*-PMMA films of (a) $16L_0$ (314 nm) and (b) $10L_0$ (196 nm) on PS-brush substrate at incident angle of 0.17°. All patterns were taken at each temperature during heating from 160 to 230 °C at a rate of 0.9 °C/min after thermally annealing the film at 170 °C for 3 days under vacuum.

to the film surface. The cross-sectional view by only the direct beam damages confirms the consistent result with the left image, though weak in the contrast.

2D GISAXS patterns for PS-*b*-PMMA film of $16L_0$ (314 nm) and $10L_0$ (196 nm) on the PS-brush substrate are shown in Figure 5a,b which were taken at the same manner during heating from 160 to 230 °C. For the GISAXS pattern of $16L_0$ film, two strong *hidden* scattering peaks along q_z near q_y = 0 are evident up to $T \approx$ 212 °C due to the parallel orientation of the lamellar microdomains to the film surface, and with increasing temperature (T > 212 °C), the *in-plane* scattering as well as two elliptical scattering is significantly intensified up to T = 230 °C, indicating the disordering of BCP films. Moreover, for the GISAXS pattern of a very thin film of $10L_0$, the *hidden* scattering peaks up to T = 214 °C weaken with further increasing temperature, and the *in-plane* scattering is intensified for T > 215 °C. An increase of transition temperature for film of $10L_0$ can be attributed to the effective interfacial interactions by the PS-brush substrate with decreasing film thickness. The numerical intensity difference of the *in-plane* scattering between the ordered and the disordered state is ~3000 a.u. for film of $40L_0$. However, with decreasing film thickness these differences come to 200 a.u. for film of $10L_0$ due to the low contrast, which hinders the transition measurement when the film thickness is less than $10L_0$.

The maximum intensity profiles of the *in-plane* scattering peaks are shown in Figure 6a as a function of temperature with

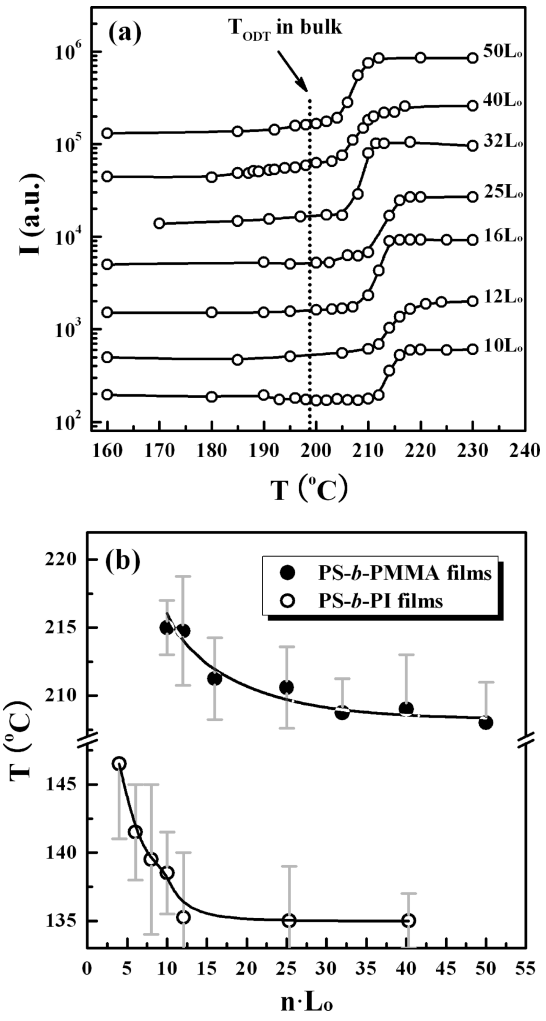

Figure 6. (a) Maximum intensity profiles of the *in-plane* scattering peaks for PS-*b*-PMMA films from $10L_0$ to $50L_0$ on the PS-brush substrate as a function of temperature, which were scanned along the q_y direction at constant $q_z = 0.263$ nm^{-1} for $10L_0$, $12L_0$, $16L_0$, $25L_0$, and $32L_0$ films and at constant $q_z = 0.269$ nm^{-1} for $40L_0$ and $50L_0$ films during heating at a rate of 0.9 °C/min. The dotted line indicates a T_{ODT} (200 °C) for the bulk PS-*b*-PMMA. (b) Thickness dependence of transition temperatures for PS-*b*-PMMA films in comparison to that for PS-*b*-PI films on the PS-brush substrate, which is reproduced from ref 23. These transition temperatures were determined at the midpoints of the discontinuous range in intensities. Error bars indicate the initial and final points of transition temperatures, and the lines serve as a guide to the eyes.

varying PS-*b*-PMMA film thickness, which were scanned along the q_y direction at constant $q_z = 0.263$ nm^{-1} for films of $10L_0$, $12L_0$, $16L_0$, $25L_0$, and $32L_0$, and at constant $q_z = 0.269$ nm^{-1} for films of $40L_0$ and $50L_0$ on the PS-brush substrate, respectively. For the film of $50L_0$ on the PS-brush substrate, an increase in intensity of *in-plane* scattering peak corresponds to the phase change from the parallel orientation of the lamellar microdomains to the film surface to a disordered state for the BCP film resulting in the correlation hole scattering, leading simply to a T_{ODT} determined at the midpoint of 208 °C. This transition temperature is the similar to those for the films of $40L_0$ and $32L_0$, while they are still above T_{ODT} (200 °C) for the bulk PS-*b*-PMMA (indicated by dotted line). As the film thickness decreases to $10L_0$, an increase of transition temperatures is observed up to a T_{ODT} = 215 °C.

The thickness dependence of transition temperatures for PS-*b*-PMMA films is shown in Figure 6b, where the experimental data points are given as closed symbols. With increasing film thickness

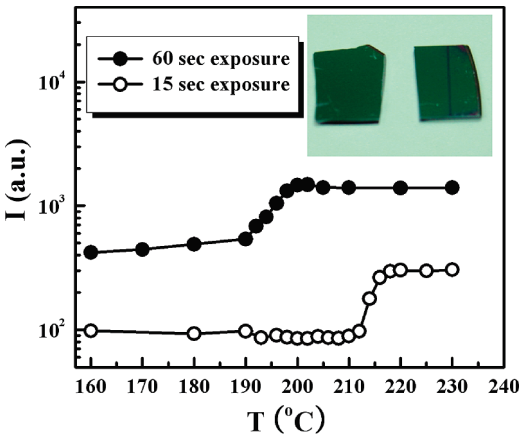

Figure 7. Maximum intensity profiles of the *in-plane* scattering peaks for PS-*b*-PMMA films of $10L_0$ on the PS-brush substrate depending on the exposure time, which were analyzed in similar manners of Figure 6. For comparison, two sample pictures after measurements are shown in the inset (the left and right pictures for the films with 15 and 60 s exposure, respectively). A dark line observed in the sample with 60 s exposure depicts the serious sample damage with long time exposure by X-rays.

up to $50L_0$, transition temperatures for PS-*b*-PMMA films gently decrease from 215 to 208 °C, whereas for PS-*b*-PI films reproduced for comparison in ref 23, they remarkably decrease to $12L_0$ and then hold the same to $40L_0$.[23] We speculate that the different behaviors of transition temperatures can be attributed presumably to the relative magnitude of temperature dependence on χ between two BCP films. A decreasing tendency of the transition temperatures for PS-*b*-PMMA films may be correlated to the weak temperature dependence of χ between two block components, presumably due to the small enthalpic contribution to χ that is inversely proportional to temperature.

Figure 7 shows the maximum intensity profiles of the *in-plane* scattering peaks for PS-*b*-PMMA films of $10L_0$ on the PS-brush substrate depending on the exposure time, which were analyzed in the similar manners of Figure 6. An unusual transition temperature (~195 °C) for the film of $10L_0$ with 60 s exposure is observed by the discontinuity in intensity, which is lower than that (215 °C) for the film with 15 s exposure. Here, we emphasize the importance of the optimum exposure time in the GISAXS measurement since the transition temperatures of PS-*b*-PMMA films may be aberrantly altered due to the serious damages by X-rays. It was observed that the transition temperatures were floating when PS-*b*-PMMA films were exposed to X-rays for long time, unlike that in the bulk state. For instance, during heating from 160 to 230 °C at a rate of 0.9 °C/min, the sample surfaces with 60 s exposure showed a dark line by the optical microscopy (OM) and the eyes. It represents that PS-*b*-PMMA films were seriously degraded with long time exposure by X-rays, as is directly seen on the right photograph in Figure 7. For the sample surfaces with less than 25 s exposure, there was no discernible damage by X-rays, as shown in the inset (the left and right pictures for the films with 15 and 60 s exposure, respectively). For this reason, the exposure time of 15 s was set to effectively minimize the degradation by X-rays because it still allows an effective intensity resolution at least within the error range of the correct transition temperature we believe.

When the propagating profiles due to the preferential interactions penetrate the film, a decay length (ξ) for the propagating profile becomes comparable to the film thickness composed of the lamellar microdomain layers. Therefore, this thickness dependence of transition temperatures can be indirectly probed by ξ with temperature change. We take the apparent transition of 208 °C for the film of $50L_0$ due to the suppressed fluctuations as a

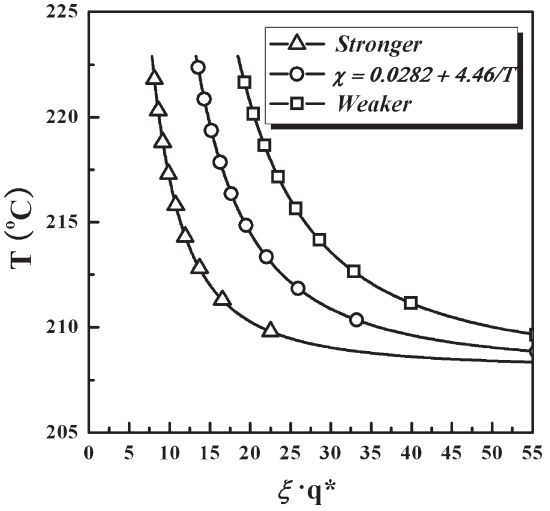

Figure 8. Theoretical transition temperature as a function of non-dimensionalized decay length (ξq^*) by employing $\chi = 0.0282 + 4.46/T$ (○) in the mean-field region. $\chi = 0.0327 + 2.322/T$ (□) with weaker and $\chi = 0.0107 + 12.92/T$ (△) with stronger enthalpic contribution are relatively compared in terms of temperature dependence of χ between block components.

starting point. For BCP films of finite thickness,[38−40] within the surface interactions, the previous theoretical study on the mean-field free energy functional suggests the effect of χ on ξ for the exponential decay of a propagating profile starting from the surfaces through the films as $\xi q^* = 2^{1/2}/[1 - (\bar{\chi}/\bar{\chi}_s)]^{1/2}$, where $\bar{\chi} \equiv 2N\chi - 2N\chi_s + \bar{\chi}_s$ with $\bar{\chi}_s = 3^{1/2}/[\phi(1-\phi)]^{3/2}$; $N\chi_s$ and q^* indicate $N\chi$ at mean-field spinodals and the equilibrium wave vector of the bulk state, respectively. On the basis of the correlation between ξq^* and nL_0, we calculated the transition temperatures as a function of ξq^* by employing $\chi = 0.0282 + 4.46/T$ in the mean-field region with a minutely adjusted molecular weight to possess the desired ODT.[25] Two modified χ's with weaker ($= 0.0327 + 2.322/T$) and stronger enthalpic contribution ($= 0.0107 + 12.92/T$), both of which yield the same hypothetical T_{ODT} at 208 °C, were also employed to clarify the effect by temperature dependence of χ between two block components, as plotted in Figure 8. Interestingly, the transition temperature of hypothetical BCP films with stronger enthalpic contribution to χ yields a drastic decrease at lower ξq^* and plateaus to a constant 208 °C, which is a similar tendency the transition temperatures for PS-*b*-PI films that possesses $\chi = -0.0419 + 38.54/T$.[35] In contrast, the transition temperature of BCP films with weaker enthalpic contribution reveals a slower (or gentle) change with increasing ξq^*. A decreasing tendency of the transition temperatures for PS-*b*-PMMA films may be correlated to the weak temperature dependence of χ between two block components, more than likely due to the small enthalpic contribution to χ that is inversely proportional to temperature. This result illustrates accordingly that the temperature dependence of χ between two block components significantly influences the thickness dependence of transition temperatures for BCP films on preferential surfaces in a good agreement with the experiments.

Conclusion

The transition behavior for the films of a weakly interacting PS-*b*-PMMA on PS-brush substrate was investigated by *in situ* GISAXS measurements by varying film thicknesses from $10L_0$ to $50L_0$. The selective interactions at the surface by PS-brush substrate that favors the preferential interactions with the PS component of the block copolymer enhance the parallel orientation of the lamellar microdomains to the film surface. The thickness dependence of transition temperatures for PS-*b*-PMMA films leads experimentally to a gentle decrease of the transition temperature with increasing film thickness up to $50L_0$ (lamellar period). However, these are still above the T_{ODT} for the bulk PS-*b*-PMMA, which can be attributed to the compositional propagation into the films and consequently to the suppression of compositional fluctuations. When the film thickness is correlated to the product of ξq^*, drastic and slower temperature dependences as a function of ξq^* can be attributed to stronger and weaker enthalpic contributions to χ, thereby leading to the characteristic thickness dependences of transition temperatures for BCP films. Hence, this remarkable difference in trend enables us to speculate the relative magnitude of enthalpic contribution to χ between two block components.

Acknowledgment. This work was supported by NRF Grant 2009-0067295 and the Nuclear R&D Programs funded by the Ministry of Education, Science & Technology (MEST), Korea. J.C. acknowledges the financial support from the GRRC program of Gyeonggi province [GRRCdankook2009-B04].

References and Notes

(1) Hamley, I. W. *The Physics of Block Copolymers*; Oxford University Press: Oxford,1998.
(2) Ruzette, A.-V.; Leibler, L. *Nat. Mater.* **2005**, *4*, 19.
(3) Hasegawa, H.; Hashimoto, T. *Macromolecules* **1985**, *18*, 589.
(4) Henkee, C. S.; Thomas, E. L.; Fetters, L. J. *J. Mater. Sci.* **1988**, *23*, 1685.
(5) Anastasiadis, S. H.; Russell, T. P.; Satija, S. K.; Majkrzak, C. F. *Phys. Rev. Lett.* **1989**, *62*, 1852.
(6) Buck, E.; Fuhrmann, J. *Macromolecules* **2001**, *34*, 2172.
(7) Mansky, P.; Liu, Y.; Huang, E.; Russell, T. P.; Hawker, C. *Science* **1997**, *275*, 1458.
(8) Huang, E.; Russell, T. P.; Harrison, C.; Chaikin, P. M.; Register, R. A.; Hawker, C. J.; Mays, J. *Macromolecules* **1998**, *31*, 7641.
(9) Huang, E.; Pruzinsky, S.; Russell, T. P.; Mays, J.; Hawker, C. J. *Macromolecules* **1999**, *32*, 5299.
(10) Ryu, D. Y.; Shin, K.; Drockenmuller, E.; Hawker, C. J.; Russell, T. P. *Science* **2005**, *308*, 236.
(11) Ham, S.; Shin, C.; Kim, E.; Ryu, D. Y.; Jeong, U.; Russell, T. P.; Hawker, C. J. *Macromolecules* **2008**, *41*, 6431.
(12) Ryu, D. Y.; Ham, S.; Kim, E.; Jeong, U.; Hawker, C. J.; Russell, T. P. *Macromolecules* **2009**, *42*, 4902.
(13) Mansky, P.; Russell, T. P.; Hawker, C. J.; Mays, J.; Cook, D. C.; Satija, S. K. *Phys. Rev. Lett.* **1997**, *79*, 237.
(14) Müller-Buschbaum, P.; Maurer, E.; Bauer, E.; Cubitt, R. *Langmuir* **2006**, *22*, 9295.
(15) Müller-Buschbaum, P.; Schulz, L.; Metwalli, E.; Moulin, J. F.; Cubitt, R. *Langmuir* **2008**, *24*, 7639.
(16) Müller-Buschbaum, P.; Schulz, L.; Metwalli, E.; Moulin, J. F.; Cubitt, R. *Langmuir* **2009**, *25*, 4235.
(17) Green, P. F.; Limary, R. *Adv. Colloid Interface Sci.* **2001**, *94*, 53.
(18) Riegler, H.; Kohler, R. *Nat. Phys.* **2007**, *3*, 890.
(19) Leibler, L. *Macromolecules* **1980**, *13*, 1602.
(20) Bates, F. S.; Fredrickson, G. H. *Annu. Rev. Phys. Chem.* **1990**, *41*, 525.
(21) Menelle, A.; Russell, T. P.; Anastasiadis, S. H.; Satija, S. K.; Majkrzak, C. F. *Phys. Rev. Lett.* **1992**, *68*, 67.
(22) Milner, S. T.; Morse, D. C. *Phys. Rev. E* **1996**, *54*, 3793.
(23) Shin, C.; Ahn, H.; Kim, E.; Ryu, D. Y.; Huh, J.; Kim, K.-W.; Russell, T. P. *Macromolecules* **2008**, *41*, 9140.
(24) Shin, C.; Ryu, D. Y.; Huh, J.; Kim, J. H.; Kim, K.-W. *Macromolecules* **2009**, *42*, 2157.
(25) Bing, M.; Dadong, Y.; Charles, C. H.; An-Chang, S. *J. Chem. Phys.* **2006**, *124*, 144902.
(26) Alexander-Katz, A.; Fredrickson, G. H. *Macromolecules* **2007**, *40*, 4075.
(27) Yoon, J.; Kim, K. W.; Kim, J.; Heo, K.; Jin, K. S.; Jin, S.; Shin, T. J.; Lee, B.; Rho, Y.; Ahn, B.; Ree, M. *Macromol. Res.* **2008**, *16*, 575.
(28) Yoon, J.; Yang, S. Y.; Lee, B.; Joo, W.; Heo, K.; Kim, J. K.; Ree, M. *J. Appl. Crystallogr.* **2007**, *40*, 305.
(29) Lee, B.; Park, I.; Yoon, J.; Park, S.; Kim, J.; Kim, K.-W.; Chang, T.; Ree, M. *Macromolecules* **2005**, *38*, 4311.
(30) Kharlampieva, E.; Kozlovskaya, V.; Tyutina, J.; Sukhishvili, S. A. *Macromolecules* **2005**, *38*, 10523.

(31) Jin, S.; Yoon, J.; Heo, K.; Park, H.-W.; Kim, J.; Kim, K.-W.; Shin, T. J.; Chang, T.; Ree, M. *J. Appl. Crystallogr.* **2007**, *40*, 950.
(32) Heo, K.; Yoon, J.; Jin, S.; Kim, J.; Kim, K.-W.; Shin, T. J.; Chung, B.; Chang, T.; Ree, M. *J. Appl. Crystallogr.* **2008**, *41*, 281.
(33) Joo, W.; Yang, S. Y.; Kim, J. K.; Jinnai, H. *Langmuir* **2008**, *24*, 12612.
(34) Zhao, Y.; Sivaniah, E.; Hashimoto, T. *Macromolecules* **2008**, *41*, 9948.
(35) Takeji, H.; Yasuhito, I.; Lewis, J. F. *J. Chem. Phys.* **1988**, *89*, 2463.
(36) Busch, P.; Rauscher, M.; Smilgies, D. M.; Posselt, D.; Papadakis, C. M. *J. Appl. Crystallogr.* **2006**, *39*, 433.
(37) Busch, P.; Posselt, D.; Smilgies, D. M.; Rauscher, M.; Papadakis, C. M. *Macromolecules* **2007**, *40*, 630.
(38) Fredrickson, G. H. *Macromolecules* **1987**, *20*, 2535.
(39) Binder, K. *Adv. Polym. Sci.* **1999**, *138*, 1.
(40) Cho, J.; Shin, K.; Cho, K. S.; Seo, Y. S.; Satija, S. K.; Ryu, D. Y.; Kim, J. K. *Macromolecules* **2008**, *41*, 955.